

Magnetic Elements Near the Solar Limb: Inversions Based on a Flux-tube Model

C. Frutiger

Institute of Astronomy, ETH Zentrum, 8092 Zürich, Switzerland

S. K. Solanki

Max-Planck-Institut für Aeronomie, 37191 Katlenburg-Lindau, Germany

A. Gandorfer

Institute of Astronomy, ETH Zentrum, 8092 Zürich, Switzerland

Abstract. We present a code for the response-function based inversion of spectra from unresolved magnetic elements that is not restricted to observations at disk centre. The inversion method is based on a multi-segmented flux-tube model that allows an efficient integration technique to be used for calculating synthetic spectra while taking into account the expanding structure of the magnetic field and a 3-dimensional velocity field in the non-magnetic surroundings of the magnetic elements.

We have applied the new inversion method to measurements of the full Stokes vector of spectral line profiles observed in an active region plage at $\mu = 0.67$. The inversion returns the stratifications of the thermodynamical quantities, such as the temperature and macroscopic velocity, as well as the properties of the magnetic field, such as the field strength, filling factor, flux-tube radius and direction (with respect to the surface normal). A comparison with results obtained from inverted FTS spectra at disk centre is promising, in particular the striking similarity between the stratifications returned by the inversions of spectra obtained at different locations.

1. Introduction

The physical structure and the dynamics of small scale magnetic elements are a key to the unified understanding of many aspects of solar (and stellar) activity. For example the brightness of facular elements plays an important role for the Sun's irradiance variations and thus the Earth's climate (Solanki 1994, Fligge et al. 2000, Fligge & Solanki 2001). An accurate knowledge of the temperature stratification of small-scale plage and network magnetic elements and their non-magnetic surroundings is important to know for all positions on the solar disk. Also, waves propagating along the flux tubes have been proposed as agents of chromospheric and coronal heating (Ulmschneider & Narain 1990, Narain & Ulmschneider 1996). In order to distinguish between the different wave modes

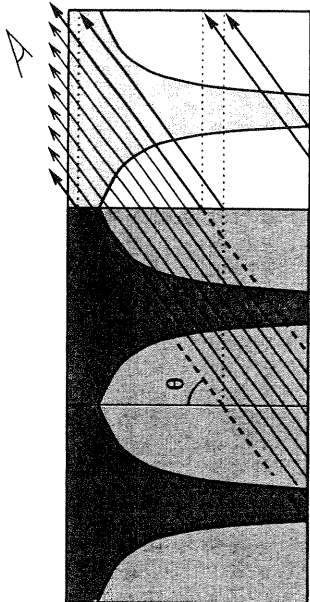


Figure 1. Flux-tube model (vertical cut): If one assumes that the flux tubes occur on a regular grid and have the same properties, then we can use a master cell to solve the radiative transfer equation along all possible lines of sight.

supported by the flux tubes it is necessary to observe them also away from disk centre (Ploner & Solanki 1997, 1999). For many purposes it is thus necessary to investigate flux tubes near the limb.

Inversion techniques based on response functions have repeatedly been shown to be a powerful means of determining the stratification of physical quantities in the solar photosphere from spectral line profiles (see, e.g., Bellot Rubio et al. 1997, Sánchez Almeida 1997, Westendorp Plaza et al. 1997, Frutiger & Solanki 1998). It is important to note, however, that these results depend on the realism of the different model atmospheres underlying the inversion. In the case of flux-tube models that take into account that the magnetic flux concentration expands with height, inversions are normally only applied to spectra obtained at disk centre.

For general positions on the disk ($\mu = \cos \theta < 1$, with θ the angle between the line-of sight and the surface normal) the standard 1.5D models (1D radiative transfer, 2D model atmosphere) are no longer adequate. The expanding structure of the magnetic field and in particular the different velocities seen by the observer must be described by a 3-dimensional model of the atmosphere under investigation. In order to obtain synthetic spectra the model atmosphere has to be sampled by a large number of rays (around 400 or more) along which the radiative transfer equations must be solved.

In the sequel we present a new flux-tube model that is able to describe the 3-dimensional structure of the magnetic flux tube and its non-magnetic surroundings and at the same time allows synthetic spectra to be calculated efficiently along many rays. The method we use is an extension of that proposed by Del Toro Iniesta et al. (1995). Savings in the computational effort become possible by dividing the atmosphere into a number of segments in which all quantities are assumed to depend only on the geometrical height in the atmosphere and by further assuming that the atmosphere consists of a regular grid of equal flux-tube cells.

2. Radiative transfer

If the angle between the line of sight and the flux-tube axis is not zero, then a particular line of sight or ray generally cuts the flux-tube boundary more than once. In addition, the symmetry around the flux-tube axis is broken with regard to the radiative transfer. Therefore a large number of rays must be used to sample the structure of the flux-tube interior and the non-magnetic surroundings in a way adequate to reproduce spatially averaged Stokes spectra. The radiative transfer equations must be solved along each of these rays, and the corresponding individual spectra must be combined to form the total synthetic spectral line profiles. If we assume that clusters of small-scale magnetic elements can be described by periodic arrays of identical, highly intermittent flux tubes, as depicted in Fig. 1, then we can solve the radiative transfer equation along any particular ray in a single master cell. A ray that cuts the boundaries of the master cell can be treated as a ray that is divided into pieces, each of which is shifted horizontally to fit into the master cell (this becomes possible due to the assumed periodicity, see thick arrows in Fig. 1).

Del Toro Iniesta et al. (1995) have presented an efficient method to solve the radiative transfer equation for a line of sight passing through two interlaced atmospheres. The concrete case they considered is of a ray passing through a atmosphere with a sharp boundary (such as created by the boundary of a flux tube). They showed that if the radiative transfer is solved for the two atmospheres on each side of the boundary separately, then the emergent radiation can be determined at very little additional computational cost for an arbitrary combination of the two atmospheres. We have extended this technique to multi-segmented atmospheres, i.e. for a ray passing through an atmosphere composed of an arbitrary number of interlaced atmospheres. We also extended their proposal to handle multiple boundaries (or transitions between one atmosphere and another) along the line of sight (see Fig. 2).

3. Flux-tube model

The full model atmosphere is composed of a number of components. The first component describes the flux-tube interior, the other component(s) either parts of the flux-tube or of the non-magnetic surroundings. The vertical stratification of the magnetic field strength, $B(z)$, and the flux-tube radius, $r(z)$, are derived from the thin-tube approximation (cf. Spruit 1981). In order to take into account that the magnetic field is rarely perpendicular to the surface (cf. Sigwarth et al. 1999), we allow the flux tube to be inclined with respect to the vertical in an arbitrary direction around the surface normal (see Fig. 2). Since we are employing the thin-tube approximation, this means that the interior of an inclined flux tube has the same (vertical) thermodynamic structure and magnetic field-strength stratification as a tube whose axis is perpendicular to the surface. The main difference is the direction of the inclined magnetic field and in particular the modified flux-tube boundary. Both affect the radiative transfer along a particular line of sight, i.e. the direction of the magnetic field with respect to the observer and the positions where the line of sight cuts the flux-tube boundary.

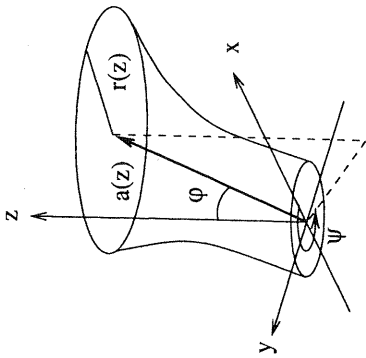


Figure 2. Reference frame used to define the flux-tube structure. The direction of the flux-tube axis (and the magnetic field vector) is given by the inclination or skew angle, φ , and the azimuthal angle, ψ (measured counter clockwise from the positive x -axis).

In order to capture both the expanding structure and the 3-dimensional properties of the surrounding velocities into a simple model we divide the atmosphere into segments in which all quantities *only* depend on the geometrical height, z (see Fig. 3). This approach allows us to take into account that the velocities seen by the observer (projected onto the line-of-sight) may strongly depend on the ray along which the radiative transfer equations are solved.

Fig. 3 shows how the atmosphere is divided into 10 volumes or segments (if we look perpendicular to the solar surface). The first segment represents the magnetic interior. A set of 8 segments describes the non-magnetic vicinity of the flux tube, while the last segment fills up the rest of the atmosphere and corresponds to the non-magnetic plasma further away. The atmospheric stratification of the segments II–IV are equal except for the direction of the macroscopic (downflow) velocities. In each of these segments the downflow is directed radially towards the flux-tube axis and parallel to the flux-tube boundary. The remaining non-magnetic surroundings harbor either no flow, or the flow is assumed to be vertical). The radial extent of these segments around the flux-tube is a function of the geometrical height. This extent relative to the flux-tube diameter is a (free) parameter of the inversions. The number of segments is arbitrary. For the inversions presented below we have chosen 8 equally spaced segments around the flux-tube.

The assumption that in each segment all quantities only depend on the geometrical height also applies for the magnetic field in the flux-tube interior. The expansion with height, however, implies that the field lines are bent and occasionally form a canopy in the upper part of the photosphere (cf. Solanki et al. 1999). Such a behavior can be described by using a model with additional segments where not only the non-magnetic vicinity is divided into segments but also the magnetic interior near the boundary (see Fig. 3). In this case the magnetic field direction in each of these new segments can be obtained for example from the first order approximation by Pneuman et al. (1986).

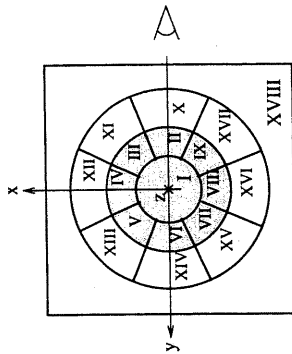


Figure 3. Horizontal cross-section through a segmented flux-tube model: In order to model the expansion of the field and downflows along the flux tube in the non-magnetic surroundings, the atmosphere is divided into 18 segments. The inner segments (grey area) correspond to the flux-tube interior while segments X–XVIII harbor a downflow pointing radially inward. The last segment is associated with the remaining surface fraction further away from the flux tube.

4. Inversion code

The new 3D model atmosphere and radiative transfer routine have been incorporated in an existing inversion code that is based on a modified Levenberg-Marquardt least squares fitting algorithm (cf. Frutiger & Solanki 1998 and Frutiger et al. 2000). The inversion returns the stratification of the temperature and line-of-sight velocity as a function of the optical depth as well as the properties of the magnetic field (field strength, field direction, filling factor, flux-tube diameter) and depth-independent quantities like the micro- and macro-turbulence.

5. Observed spectra and atomic data

We have used observations of an active region at $\mu = 0.67$ obtained with the ZIMPOL II polarimeter (cf. Gandorfer & Povel 1997) and the Gregory-Coudé telescope at IRSOL, Locarno. Since Q/I , U/I and V/I are the output of the ZIMPOL device we have directly fitted these profiles and not used Q/I_c , U/I_c and V/I_c which would have required an additional preprocessing step and occasionally introduced small errors due to inaccuracies in the determination of the true continuum intensity I_c . The spatial resolution of the observed spectra is about 2 arc seconds (limited by seeing conditions). The spectral resolution was chosen to be about 300000.

6. First results

In order to verify that our new segmented flux-tube model atmosphere and the new integration method for the calculation of the synthetic spectra gives

reasonable results we have compared the stratifications returned by the inversion with those obtained from FTS spectra at disk centre (Frutiger & Solanki 2000).

The best-fit atmospheric stratifications returned by the inversion are shown in Fig. 6. The comparison with the results returned from inverted FTS data of a plage close to disk-centre (cf. Frutiger & Solanki 2000) is striking. This is particularly true if one takes into account that the spatial resolution of the FTS measurements is only 10 arc seconds, i.e. they cover an area on the solar surface that is about 10 times larger than the area observed with the ZIMPOL instrument. Clearly, the full Stokes vector of the four Fe I lines carries the necessary information to derive the stratifications of the temperature, the line-of-sight velocity and the properties of the magnetic field. In our particular case the axis of the flux tube turned out to be slightly inclined to the vertical by an angle of $\varphi = 4.1 \pm 1.3$ deg and rotated by an angle of $\psi = 21 \pm 20$ deg. In our model we assumed a depth independent velocity in the flux-tube interior for which the inversion returned an almost vanishingly small upflow. The large differences between the microturbulence at disk centre and the limb in the field-free atmosphere is qualitatively consistent with the results of Holweger et al. (1978) and Frutiger et al. (2000) obtained from quiet-Sun data.

7. Conclusions

The first results obtained from the inversion of plage data at $\mu = 0.67$, i.e. away from solar disk centre, shows that the new multi-segmented flux-tube model underlying the inversion is promising, not only as far as speed is concerned. The almost perfect match with results obtained from inverted FTS spectra at disk centre shows that the inversion is able to derive the full stratification of physical quantities like the temperature, line-of-sight velocity or the properties of the magnetic field from a small set of spectral absorption lines for which the full Stokes vector has been measured. The future application of the new inversion code allows spectra to be analyzed at any position on the Sun. This will hopefully help to gain more insights in the structure of as yet unresolved magnetic plage and network elements.

References

- Bellot Rubio, L. R., Ruiz Cobo, B., & Collados, M. 1997, ApJ 478, L45
 Del Toro Iniesta, J. C., Ruiz Cobo, B., Bellot Rubio, L. R., & Collados, M. 1995, A&A 294, 855
 Fligge, M., & Solanki, S. K. 2001, J. Astrophys. Astr., in press
 Fligge, M., Solanki, S. K., & Unruh, Y. C. 2000, A&A 353, 380
 Frutiger, C., & Solanki, S. K. 1998, A&A 336, L65
 Frutiger, C., & Solanki, S. K. 2000, A&A, submitted
 Frutiger, C., Solanki, S. K., Fligge, M., & Bruls, J. H. M. J. 2000, A&A 358, 1109
 Gandorfer, A. M., & Povel, H. P. 1997, A&A 328, 381
 Holweger, H., Gehlsen, M., & Ruland, F. 1978, A&A 70, 537

- Narain, U., & Ulmschneider, P. 1996, *Space Sci. Rev.* 75, 453
 Ploner, S. R. O., & Solanki, S. K. 1997, *A&A* 325, 1199
 — 1999, *A&A* 345, 986
 Pneuman, G. W., Solanki, S. K., & Stenflo, J. O. 1986, *A&A* 154, 231
 Sánchez Almeida, J. 1997, *ApJ* 491, 993
 Sigwarth, M., Balasubramaniam, K. S., Knölker, M., & Schmidt, W. 1999, *A&A* 349, 941
 Solanki, S. K. 1994, in *The Sun as a Variable Star: Solar and Stellar Irradiance Variations*, ed. J. M. Pap, C. Fröhlich, H. S. Hudson & S. K. Solanki (Cambridge: Cambridge Univ. Press), 226
 Solanki, S. K., Finsterle, W., Rüedi, I., & Livingston, W. 1999, *A&A* 347, L27
 Spruit, H. C. 1981, *A&A* 102, 129
 Ulmschneider, P., & Narain, U. 1990, in *IAU Symp. 142: Basic Plasma Processes on the Sun*, ed. E. R. Priest & V. Krishan (Kluwer Academic Publishers), 97
 Westendorp Plaza, C., del Toro Iniesta, J. C., Ruiz Cobo, B., et al. 1997, *Nature* 389, 47

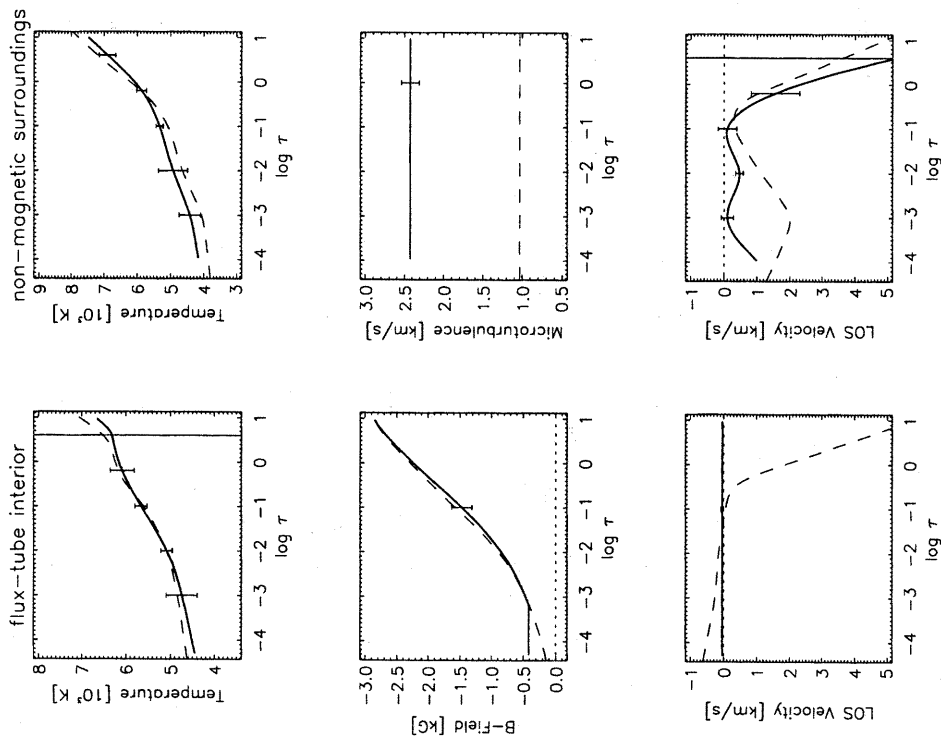


Figure 4. Best-fit stratifications returned by inversions of spectra obtained at $\mu = 0.67$ (solid) and at disk centre (dashed). The frames in the left column show the physical quantities in the flux-tube interior, the frames in the right column those in the non-magnetic surroundings. Error bars are plotted at the optical depths at which free parameters are located (the vertical line at $\log \tau = 0.6$ in some of the frames is due to error bars that extend beyond the frame).